International Journal of Heat and Mass Transfer 52 (2009) 2902–2913

Contents lists available at ScienceDirect

International Journal of Heat and Mass Transfer

journal homepage: www.elsevier.com/locate/ijhmt

Flow and heat transfer in a power-law fluid over a stretching sheet with variable thermal conductivity and non-uniform heat source

M. Subhas Abel [a,*], P.S. Datti [b], N. Mahesha [a]

[a] Department of Mathematics, Gulbarga University, Gulbarga, Karnataka, India
[b] TIFR Centre, Indian Institute of Science Campus, Bangalore, Karnataka, India

ARTICLE INFO

Article history:
Received 16 June 2008
Received in revised form 30 July 2008
Available online 14 February 2009

Keywords:
Power-law fluid
Stretching sheet
Variable thermal conductivity
Non-uniform heat source
Prandtl number

ABSTRACT

In this paper the flow of a power-law fluid due to a linearly stretching sheet and heat transfer characteristics using variable thermal conductivity is studied in the presence of a non-uniform heat source/sink. The thermal conductivity is assumed to vary as a linear function of temperature. The similarity transformation is used to convert the governing partial differential equations of flow and heat transfer into a set of non-linear ordinary differential equations. The Keller box method is used to find the solution of the boundary value problem. The effect of power-law index, Chandrasekhar number, Prandtl number, non-uniform heat source/sink parameters and variable thermal conductivity parameter on the dynamics is analyzed. The skin friction and heat transfer coefficients are tabulated for a range of values of said parameters.

1. Introduction

The study of laminar boundary layer flow and heat transfer in a non-Newtonian fluid over a stretching sheet, issuing from a slit, has gained tremendous interest in the past two decades. A great number of investigations concern the boundary layer behavior on a stretching surface and this is important in many engineering and industrial applications. Flow due to stretching sheet is often encountered in extrusion processes (Fig. 1) where a melt is stretched into a cooling liquid. Apart from this, many metallurgical processes including chemical engineering processes involve cooling of continuous stripes or filaments by drawing them into a cooling system. The fluid mechanical properties desired for the outcome of such a process would mainly depend on the rate of cooling and stretching rate. So, one has to pay considerable attention in knowing the heat transfer characteristics of the stretching sheet as well.

In view of many such applications (see [13]) Crane [1] initiated the analytical study of boundary layer flow due to a stretching sheet. The velocity of the sheet was assumed to vary linearly with the distance from the slit. The work of Crane was subsequently extended by many authors to Newtonian/non-Newtonian boundary layer flow with various velocity and thermal boundary conditions; see, for example, Gupta and Gupta [2], Chen and Char [3], Grubka and Bobba [4], Chiam [5,19,20], Andersson et al. [8,12,31], Siddheshwar and Mahabaleshwar [13], Abel et al. [21,27,28], Liao [29,30], Rajagopal et al. [32] and references therein.

Gupta and Gupta [2] investigated heat transfer from an isothermal stretching sheet with suction/blowing effects. Chen and Char [3] extended the works of Gupta and Gupta [2] to that of a non-isothermal stretching sheet. Grubka and Bobba [4] carried out heat transfer studies by considering the power law variation of surface temperature. Chiam [5] investigated the magnetohydrodynamic heat transfer from a non-isothermal stretching sheet. These studies concern only Newtonian fluids. However, most of the practical situations demand for fluids that are non-Newtonian in nature which are extensively used in many industrial and engineering applications. Acrivos et al. [6] investigated momentum and heat transfer in laminar boundary layer flow of non-Newtonian fluids past external surfaces. Schowalter [7] applied boundary layer theory to study flow of power-law pseudo-plastic fluids and obtained similar solutions. Andersson et al. [8] studied the flow of a power-law fluid over a stretching sheet. Mahmoud and Mahmoud [9] obtained analytical solutions of hydromagnetic boundary layer flow of a power-law fluid past a continuously moving surface. Hassanien et al. [10] investigated the flow and heat transfer in a power-law fluid over a non-isothermal stretching sheet with suction/injection.

An electrically conducting cooling fluid flow can be regulated by an external magnetic field and thereby the heat transfer rate can also be controlled. With this point of view Sarpakaya [11] has investigated the effect of magnetic field on flow of non-Newtonian fluid. Andersson [12] examined the influence of uniform magnetic field on the motion of an electrically conducting viscoelastic fluid over a stretching sheet. Siddeshwar and Mahabaleshwar [13] studied the influence of magnetic field on the flow and heat transfer in a viscoelastic fluid in the presence of uniform heat source and thermal radiation. Abo-Eldahab and Salem [14] studied the influence of

* Corresponding author. Tel.: +91 8472 245633.
E-mail address: msabel2001@yahoo.co.uk (M.S. Abel).

0017-9310/$ - see front matter © 2008 Elsevier Ltd. All rights reserved.
doi:10.1016/j.ijheatmasstransfer.2008.08.042

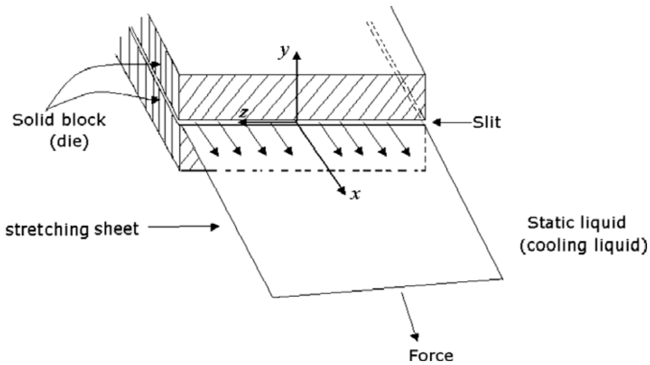

Fig. 1. Schematic of an extrusion process [13].

transverse magnetic field on the flow and heat transfer of an electrically conducting power-law fluid over a stretching sheet with a uniform free stream. An excellent work on magnetohydrodynamic stretching sheet problem involving a power-law fluid has been reported by Liao [30] using the homotopy based analytical method.

As the study of heat source/sink effect on heat transfer is very important in view of several physical problems, Vajravelu and Rollins [15] and Vajravelu and Nayfeh [16] studied flow due to a stretching surface and heat transfer in presence of uniform heat source/sink (temperature-dependent heat source/sink). Abo-Eldahab and El-Aziz [17] included the effect of non-uniform heat source/sink (space- and temperature-dependent heat source/sink) with suction/blowing. But these works are confined to viscous fluids only. Recently, Abel et al. [27,28] extended the work of Abo-Eldahab and El-Aziz [17] to that of a viscoelastic fluid.

The above-cited works concern constant physical properties for the cooling liquid, but practical situations demand for physical properties with variable characteristics. Thermal conductivity is one such property, which is assumed to vary linearly with the temperature [18]. Chiam [19,20] considered the effect of variable thermal conductivity on heat transfer. Abel et al. [21] have studied the effect of variable thermal conductivity on the MHD boundary layer viscoelastic fluid flow with temperature-dependent heat source/sink, in presence of thermal radiation and buoyancy force.

Motivated by all these works we propose to investigate the effects of variable thermal conductivity, non-uniform heat source on the flow and heat transfer in an electrically conducting power-law fluid over a stretching sheet, in presence of an external transverse magnetic field. In studying the heat transfer characteristics, two different types of boundary conditions are considered.

2. Mathematical formulation

We consider the steady two-dimensional flow of an incompressible, electrically conducting, non-Newtonian power-law fluid obeying Ostwald-de Waele model over a flat impermeable stretching sheet. The flow is generated by the action of two equal and opposite forces along the x-axis and the sheet is stretched with a velocity that is proportional to the distance from the origin (Fig. 2). The flow field is subjected to a transverse uniform magnetic field of strength H_0 and it is assumed that the induced magnetic field is negligibly small (small magnetic Reynolds number limit).

The non-Newtonian fluid model used for the present analysis is the two-parameter power-law model of Ostwald-de Waele with the parameters defined by Bird et al. [22]:

$$\tau = \left(K \left| \sqrt{\frac{\Delta.\Delta}{2}} \right|^{n-1} \right) \Delta, \tag{1}$$

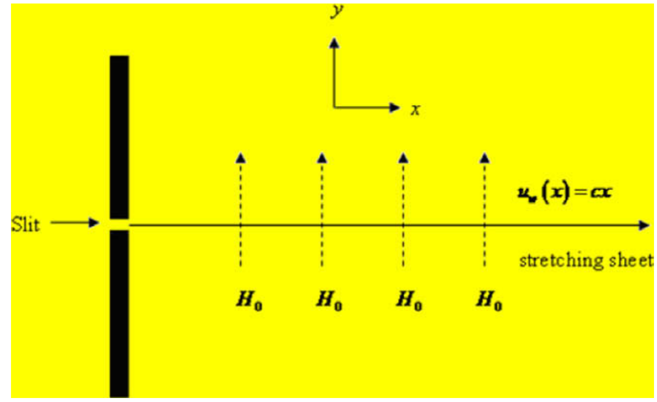

Fig. 2. Schematic of a two-dimensional stretching sheet problem.

where τ is the stress tensor, Δ is the rate of deformation of symmetric tensor, K is the consistency coefficient, and n is the power-law index. The above power-law model represents Newtonian fluid when $n = 1$, with the dynamic coefficient of viscosity K. If $n < 1$ the fluid is said to be pseudo-plastic (shear thinning fluids) and if $n > 1$ it is called dilatant (shear thickening fluids). The shear stress component of the stress tensor for power-law fluid takes (see [22]) the following form:

$$\tau_{xy} = K \left| \frac{\partial u}{\partial y} \right|^{n-1} \frac{\partial u}{\partial y}. \tag{2}$$

Now, the boundary layer equations governing the flow and heat transfer in a power-law fluid over a stretching sheet, assuming that the viscous dissipation is negligible, are given by

$$\frac{\partial u}{\partial x} + \frac{\partial v}{\partial y} = 0, \tag{3}$$

$$u\frac{\partial u}{\partial x} + v\frac{\partial u}{\partial y} = \frac{1}{\rho}\frac{\partial \tau_{xy}}{\partial y} - \frac{\sigma H_0^2 u}{\rho}, \tag{4}$$

$$u\frac{\partial t}{\partial x} + v\frac{\partial t}{\partial y} = \frac{\partial}{\partial y}\left(\frac{k}{\rho C_p}\frac{\partial t}{\partial y}\right) + \frac{q'''}{\rho C_p}, \tag{5}$$

where u and v are the velocity components along x and y directions, respectively, t is the temperature of the fluid, ρ is the density, σ is the electrical conductivity of the fluid, τ_{xy} is the shear stress given by (2), C_p is the specific heat at constant pressure, k is the thermal conductivity which is assumed to vary linearly with temperature and it is of the form, $k = k_\infty\left[1 + \varepsilon\left(\frac{t - t_\infty}{t_w - t_\infty}\right)\right]$ with ε being a small parameter. The non-uniform heat source/sink q''' is modeled as (see [17])

$$q''' = \frac{\rho k u_w(x)}{xK}[A^*(t_w - t_\infty)f' + (t - t_\infty)B^*], \tag{6}$$

where A^* and B^* are the coefficients of space- and temperature-dependent heat source/sink, respectively. Here we make a note that the case $A^* > 0, B^* > 0$ corresponds to internal heat generation and that $A^* < 0, B^* < 0$ corresponds to internal heat absorption.

We have adopted the following two kinds of boundary heating:

(i) prescribed power-law surface temperature (PST)

$$u = u_w = cx, \quad v = 0, \quad t = t_w = t_\infty + A\left(\frac{x}{L}\right)^\lambda \quad \text{at } y = 0,$$
$$u \to 0, \quad t \to t_\infty \quad \text{as } y \to \infty, \tag{7}$$

(ii) prescribed power-law heat flux (PHF)

$$u = u_w = cx, \quad v = 0, \quad -k\frac{\partial t}{\partial y} = q_w = D\left(\frac{x}{L}\right)^{\lambda+((1-n)/(1+n))} \quad \text{at } y = 0,$$
$$u \to 0, t \to t_\infty \quad \text{as } y \to \infty, \tag{8}$$

where t_w is the temperature of the sheet, t_∞ is the temperature of the fluid far away from the sheet, A and D are constants, λ is the temperature parameter and L is the characteristic length.

We introduce the following dimensionless variables:

$$X = \frac{x}{L}, \quad Y = \left(\frac{\rho U_0^{2-n} L^n}{K}\right)^{\frac{1}{n+1}} \frac{y}{L}, \quad U = \frac{u}{U_0},$$
$$V = \left(\frac{\rho U_0^{2-n} L^n}{K}\right)^{\frac{1}{n+1}} \frac{v}{U_0}, \quad T = \frac{t - t_\infty}{t_w - t_\infty},$$
$$\tau_{XY} = \left|\frac{\partial U}{\partial Y}\right|^{n-1} \frac{\partial U}{\partial Y} = \left(\frac{K U_0^{3n} \rho^n}{L^n}\right)^{\frac{-1}{n+1}} \tau_{xy}, \quad Re_L = \frac{\rho U_0^{2-n} L^n}{K},$$

where $U_0 = cL$ is the reference velocity and $t_w - t_\infty = \left\{\begin{array}{ll} AX^\lambda & \text{in PST} \\ \frac{DL}{k_\infty} Re_L^{-1/(n+1)} X^\lambda & \text{in PHF} \end{array}\right\}$.

The boundary layer equations (3)–(5) now take the following form:

$$\frac{\partial U}{\partial X} + \frac{\partial V}{\partial Y} = 0, \tag{9}$$
$$U\frac{\partial U}{\partial X} + V\frac{\partial U}{\partial Y} = \frac{\partial}{\partial Y}\left(\left|\frac{\partial U}{\partial Y}\right|^{n-1} \frac{\partial U}{\partial Y}\right) - QU, \tag{10}$$
$$U\frac{\partial T}{\partial X} + V\frac{\partial T}{\partial Y} + \frac{\lambda T U}{X} = \frac{1}{Pr_L}\left\{(1+\varepsilon T)\frac{\partial^2 T}{\partial Y^2} + \varepsilon\left(\frac{\partial T}{\partial Y}\right)^2\right\} + (1+\varepsilon T)(\alpha f' + \beta T), \tag{11}$$

where $Q = \frac{\sigma H_0^2}{\rho c}$ is the Chandrasekhar number, $Pr_L = \frac{\rho C_p U_0 L}{k_\infty (Re_L)^{2/(n+1)}}$ is the uniform Prandtl number, $\alpha = \frac{k_\infty A^*}{K C_p}$ is the space dependent heat source/sink parameter and $\beta = \frac{k_\infty B^*}{K C_p}$ is the temperature dependent heat source/sink parameter.

The boundary conditions (7) and (8) put together takes the form

$$U = U_w = X, \quad V = 0, \quad \left\{\begin{array}{ll} T = 1 & \text{in PST} \\ \frac{\partial T}{\partial Y} = -\frac{X^{(1-n)/(1+n)}}{1+\varepsilon T} & \text{in PHF} \end{array}\right\} \text{ at } Y = 0, \tag{12}$$
$$U \to 0, \quad T \to 0 \quad \text{as } Y \to \infty.$$

Introducing the stream function $\psi(X, Y)$ so as to satisfy the continuity equation in the dimensionless form (9), we have

$$U = \frac{\partial \psi}{\partial Y}, \quad V = -\frac{\partial \psi}{\partial X}. \tag{13}$$

Using (13), Eqs. (10) and (11), with the boundary conditions (12), can be written as

$$\frac{\partial \psi}{\partial Y}\frac{\partial^2 \psi}{\partial X \partial Y} - \frac{\partial \psi}{\partial X}\frac{\partial^2 \psi}{\partial Y^2} = \frac{\partial}{\partial Y}\left(\left|\frac{\partial^2 \psi}{\partial Y^2}\right|^{n-1} \frac{\partial^2 \psi}{\partial Y^2}\right) - Q\frac{\partial \psi}{\partial Y}, \tag{14}$$
$$\frac{\partial \psi}{\partial Y}\frac{\partial T}{\partial X} - \frac{\partial \psi}{\partial X}\frac{\partial T}{\partial Y} + \frac{\lambda T}{X}\frac{\partial \psi}{\partial Y} = \frac{1}{Pr_L}\left\{(1+\varepsilon T)\frac{\partial^2 T}{\partial Y^2} + \varepsilon\left(\frac{\partial T}{\partial Y}\right)^2\right\} + (1+\varepsilon T)(\alpha f' + \beta T), \tag{15}$$
$$\frac{\partial \psi}{\partial Y} = X, \quad \frac{\partial \psi}{\partial X} = 0, \left\{\begin{array}{ll} T = 1 & \text{in PST} \\ \frac{\partial T}{\partial Y} = -\frac{X^{(1-n)/(1+n)}}{1+\varepsilon T} & \text{in PHF} \end{array}\right\} \text{ at } Y = 0, \tag{16}$$
$$\frac{\partial \psi}{\partial Y} \to 0, \quad T \to 0 \quad \text{as } Y \to \infty.$$

In order to convert the partial differential equations (14) and (15) into ordinary differential equations the following similarity transformation is adopted:

$$\psi(X, Y) = X^{\frac{2n}{n+1}} f(\eta), \quad T(X, Y) = \left\{\begin{array}{ll} \theta(\eta) & \text{in PST} \\ g(\eta) & \text{in PHF} \end{array}\right\}, \quad \eta = X^{\frac{1-n}{1+n}} Y. \tag{17}$$

Using (17), Eq. (14) can be written as

$$(|f''|^{n-1} f'')' - f'^2 + \left(\frac{2n}{n+1}\right) f f'' - Qf' = 0, \tag{18}$$

where the prime denotes differentiation with respect to the similarity variable η. It is assumed that for the flow next to stretching surface $\frac{\partial u}{\partial y} \leqslant 0$, i.e., $f'' \leqslant 0$. Hence Eq. (18) further simplifies to

$$n(-f'')^{n-1} f''' - f'^2 + \left(\frac{2n}{n+1}\right) f f'' - Qf' = 0. \tag{19}$$

On using (17) in Eqs. (15) and (16), along with Eq. (19), we obtain the following boundary value problems

(i) PST:

$$n(-f'')^{n-1} f''' - f'^2 + \left(\frac{2n}{n+1}\right) f f'' - Qf' = 0, \tag{20}$$
$$(1+\varepsilon\theta)\theta'' + Pr_x\left\{\left(\frac{2n}{n+1}\right) f\theta' - \lambda f'\theta\right\} + Pr_x(1+\varepsilon\theta)(\alpha f' + \beta\theta) + \varepsilon\theta'^2 = 0, \tag{21}$$
$$f(\eta) = 0, \quad f'(\eta) = 1, \quad \theta(\eta) = 1 \quad \text{at } \eta = 0,$$
$$f'(\eta) \to 0, \quad \theta(\eta) \to 0 \quad \text{as } \eta \to \infty, \tag{22}$$

(ii) PHF:

$$n(-f'')^{n-1} f''' - f'^2 + \left(\frac{2n}{n+1}\right) f f'' - Qf' = 0, \tag{23}$$
$$(1+\varepsilon g)g'' + Pr_x\left\{\left(\frac{2n}{n+1}\right) f g' - \lambda f' g\right\} + Pr_x(1+\varepsilon g)(\alpha f' + \beta g) + \varepsilon g'^2 = 0, \tag{24}$$
$$f(\eta) = 0, \quad f'(\eta) = 1, \quad g'(\eta) = \frac{-1}{1+\varepsilon g(\eta)} \quad \text{at } \eta = 0,$$
$$f'(\eta) \to 0, \quad g(\eta) \to 0 \quad \text{as } \eta \to \infty, \tag{25}$$

where $Pr_x = \frac{\rho C_p u_w x}{k_\infty (Re_x)^{2/(n+1)}}$ is the generalized Prandtl number.

The local skin friction coefficient C_f and the local Nusselt number Nu_x at the wall are given by:

$$C_f = -2Re_x^{-1/n+1}[-f''(0)]^n, \tag{26}$$
$$Nu_x = \left\{\begin{array}{ll} -Re_x^{1/n+1}\theta'(0) & \text{in PST} \\ -Re_x^{1/n+1} g'(0) & \text{in PHF,} \end{array}\right. \tag{27}$$

where $Re_x = \frac{\rho u_w^{2-n} x^n}{K}$ is the local Reynolds number. In what follows, we drop the subscript x for the sake of simplicity, when referring to the non-dimensional parameters like Prandtl and Reynolds numbers.

We now outline the procedure for solving the boundary value problems (20)–(22) and (23)–(25).

3. Method of solution

We use Keller Box method (see [25]) in finding the numerical solutions of the resulting boundary value problems. Usually this method is associated with numerical solutions of partial differential equations. In the present context we use this method to solve system of ordinary differential equations. To solve the boundary value problems by the Keller box method Eqs. (20) and (21) in the PST case are transformed into a system of five first order differential equations as follows:

$$\begin{aligned}
\frac{df_0}{d\eta} &= f_1, \\
\frac{df_1}{d\eta} &= f_2, \\
\frac{df_2}{d\eta} &= \frac{1}{n}(-f_2)^{1-n}\left\{f_1^2 - \left(\frac{2n}{n+1}\right)f_0 f_2 + Qf_1\right\}, \\
\frac{d\theta_0}{d\eta} &= \theta_1, \\
\frac{d\theta_1}{d\eta} &= \frac{1}{1+\varepsilon\theta_0}\left\{\lambda Prf_1\theta_0 - \left(\frac{2n}{n+1}\right)Prf_0\theta_1 - \varepsilon\theta_1^2\right\} - Pr(\alpha f_1 + \beta\theta_0).
\end{aligned} \tag{28}$$

Subsequently the boundary conditions (22) take the form

$$\begin{aligned}
&f_0(0) = 0, \quad f_1(0) = 1, \quad \theta_0(0) = 1, \\
&f_1(\infty) = 0, \quad \theta_0(\infty) = 0,
\end{aligned} \tag{29}$$

where $f_0 = f(\eta)$, and $\theta_0 = \theta(\eta)$. The resulting system of equations (28) is transformed into a system of non-linear algebraic equations (finite difference equations) using a central difference scheme with uniform mesh points. The boundary conditions in (29) form a part of the system of finite difference equations. The transformed system of non-linear algebraic equations is then linearized by Newton's method. This system of linear algebraic equations is then solved by the Gauss elimination method. Shooting method (see [24]) is used to obtain the initial guess solution for the Keller box method. Same procedure is adopted to solve the boundary layer Eqs. (23) and (24) subjected to the conditions (25) in the PHF case. The results are presented in several tables and graphs. In the next section we consider the special case of a Newtonian problem ($n = 1$) to ascertain the validity of results.

4. Analytical solution for Newtonian problem (*n* = 1)

4.1. Solution for momentum equation

The momentum boundary layer Eq. (19) reduces to

$$f''' - f'^2 + ff'' - Qf' = 0, \tag{30}$$

with boundary conditions

$$\begin{aligned}
&f(\eta) = 0, \quad f'(\eta) = 1, \quad \text{at } \eta = 0, \\
&f'(\eta) \to 0, \quad \text{as } \eta \to \infty.
\end{aligned} \tag{31}$$

The momentum boundary layer Eq. (30) subjected to the boundary conditions (31) has an exact solution (see Pavlov [33]) of the form

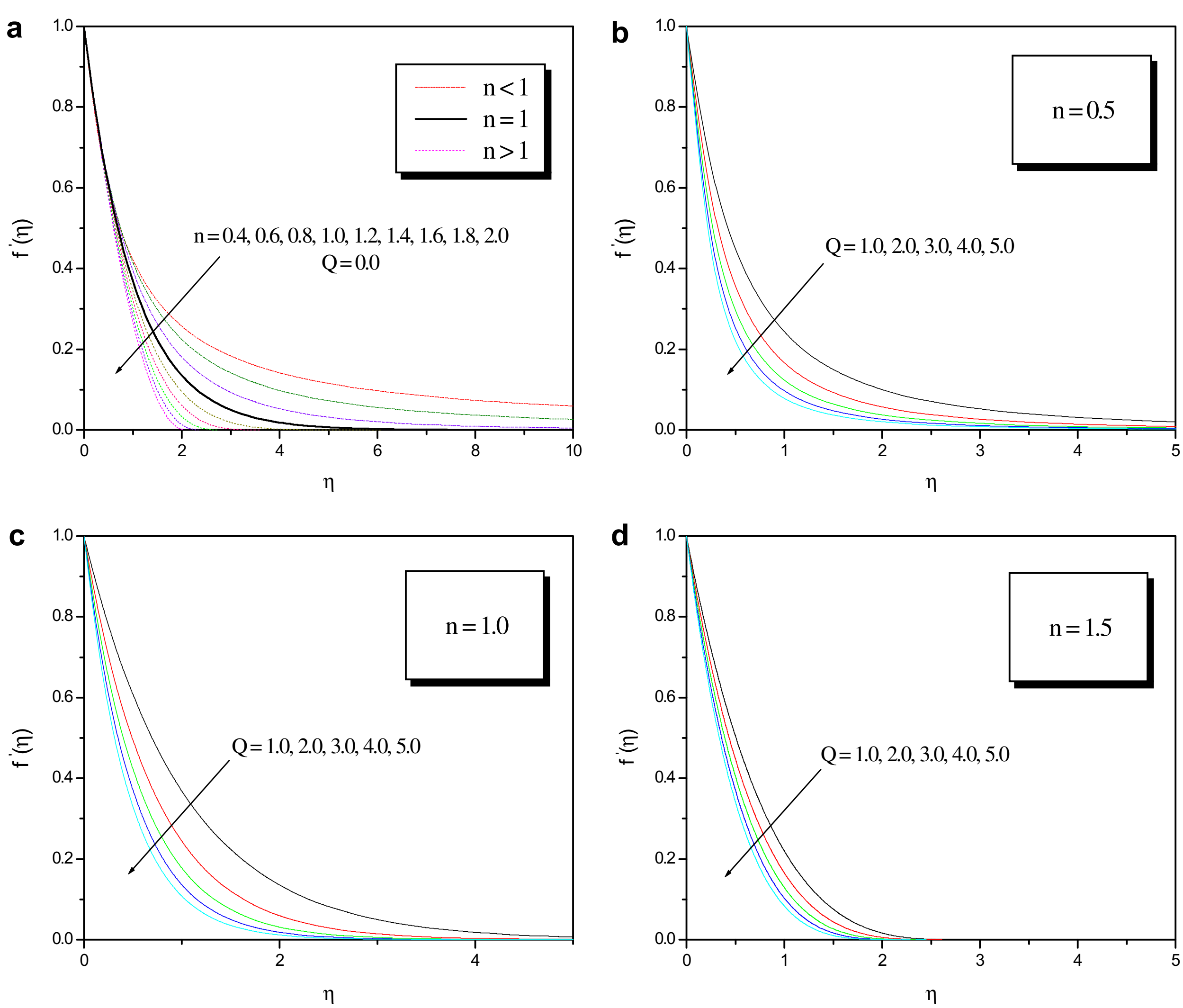

Fig. 3. Effect of power-law index n and Chandrasekhar number Q on horizontal velocity profiles.

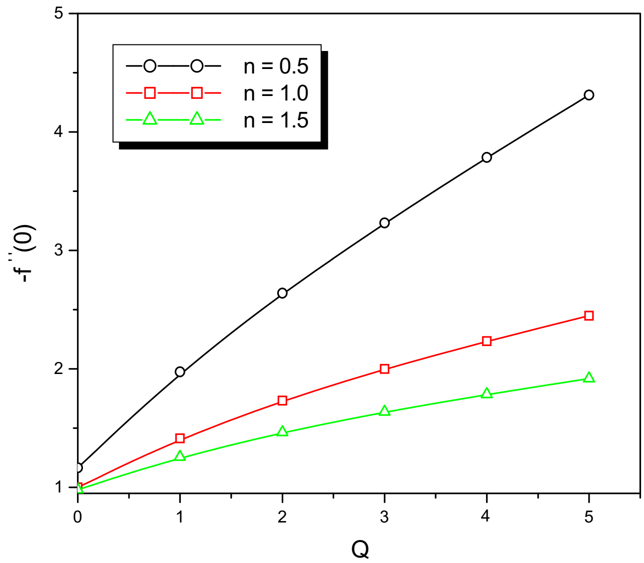

Fig. 4. Effect of Chandrasekhar number Q on $f''(0)$ for different values of n.

$$f(\eta) = \frac{1 - e^{-m\eta}}{m}, \tag{32}$$

where $m = \sqrt{1+Q}$. (33)

4.2. Solution for heat equation

The presence of a small parameter ε in the thermal boundary layer equation enables us to seek its solution through the perturbation method.

4.2.1. PST case

Consider the heat transfer equation in PST case in the form,

$$(1+\varepsilon\theta)\theta'' + Pr(f\theta' - \lambda f'\theta) + Pr(1+\varepsilon\theta)(\alpha f' + \beta\theta) + \varepsilon\theta'^2 = 0, \tag{34}$$

with boundary conditions

$$\theta(\eta) = 1, \quad \text{at } \eta = 0,$$
$$\theta(\eta) \to 0 \quad \text{as } \eta \to \infty. \tag{35}$$

The solution of Eq. (34) is assumed in the form,

$$\theta(\eta) = \theta_0(\eta) + \varepsilon\theta_1(\eta) + \varepsilon^2\theta_2(\eta) + \cdots \tag{36}$$

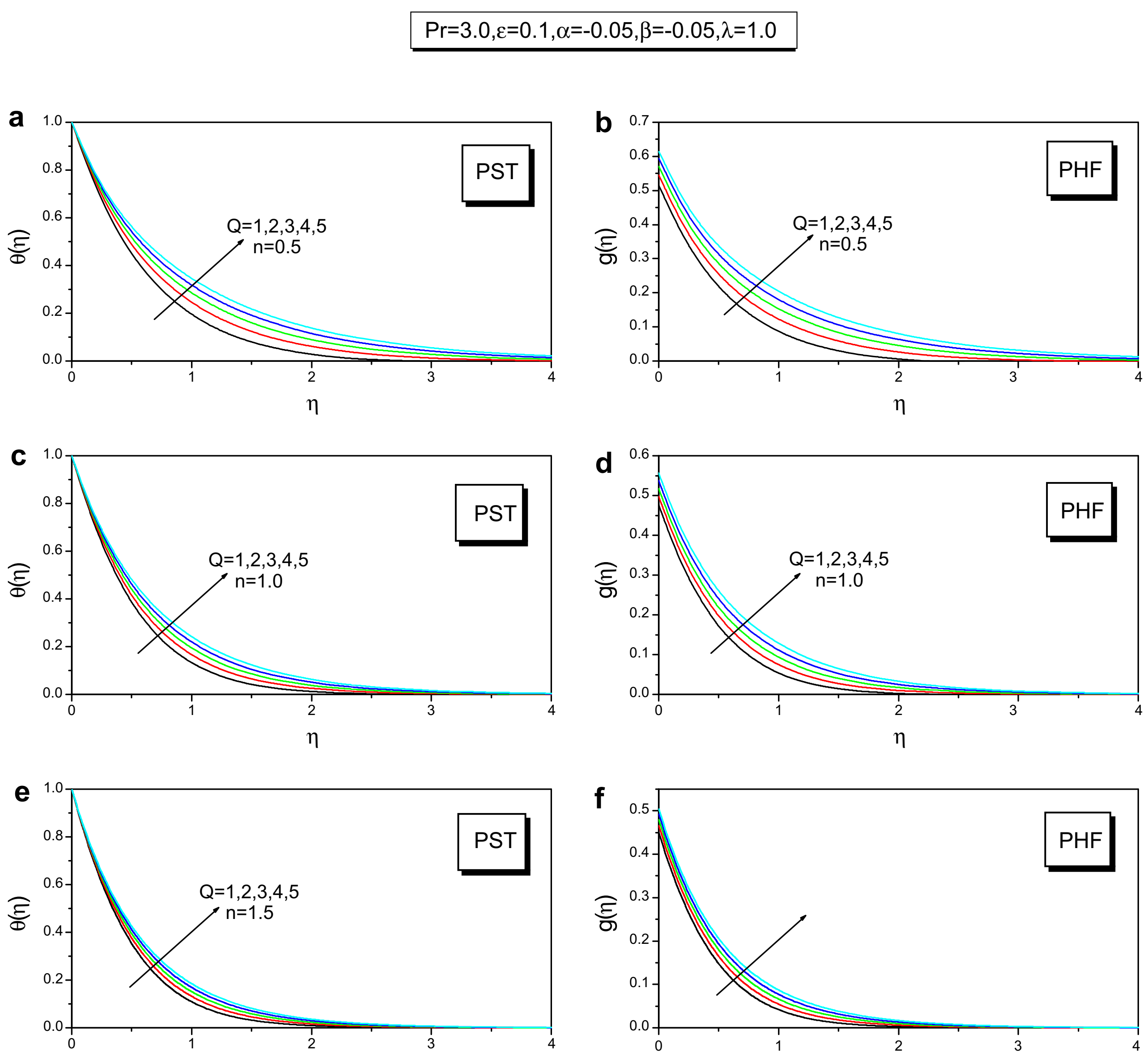

Fig. 5. Effect of Chandrasekhar number Q on temperature profiles.

Following the procedure of perturbation method the solution of the zeroth order perturbation equation is obtained in terms of Kummer's function (see [23]) as follows:

$$\theta_0(\eta)=\mathbb{C}_1 e^{-m\gamma\eta}M[\gamma-\lambda,b+1,-ae^{-m\eta}] + \left(\frac{\alpha}{1-a+a\beta}\right)\sum_{i=0}^{\infty}\left(\prod_{j=1}^{i}\frac{j-\lambda}{(j+1)^2-a(j+1)+a\beta}\right)(-a)^{i+1}e^{-m(i+1)\eta} \tag{37}$$

Using the above, the solution of the first order perturbation equation is obtained in the form,

$$\begin{aligned}\theta_1(\eta) = {} & \mathbb{C}_2 e^{-m\gamma\eta}M[\gamma-\lambda,b+1,-ae^{-m\eta}] \\ & + \{\tilde{a}_0 a^2 e^{-2m\eta} - \tilde{a}_1 a^3 e^{-3m\eta} + \tilde{a}_2 a^4 e^{-4m\eta} - \cdots\} \\ & + \mathbb{C}_1 e^{-m\gamma\eta}\{-\tilde{b}_0 a e^{-m\eta} + \tilde{b}_1 a^2 e^{-2m\eta} - \tilde{b}_2 a^3 e^{-3m\eta} + \cdots\} \\ & + \mathbb{C}_1^2 e^{-2m\gamma\eta}\{\tilde{c}_0 - \tilde{c}_1 a e^{-m\eta} + \tilde{c}_2 a^2 e^{-2m\eta} - \cdots\}.\end{aligned} \tag{38}$$

Similarly $\theta_2(\eta)$ is obtained. The solution thus obtained for small ε is uniformly valid, because the higher order terms are too small in magnitude as compared to the dominant zeroth order term. The higher order terms beyond the second order act as a mere correction factor and further enhances complexity in computation. These factors for small ε suggest quitting perturbation at this stage. Finally the solution is written as,

$$\theta(\eta) = \theta_0(\eta) + \varepsilon\theta_1(\eta) + \varepsilon^2\theta_2(\eta), \tag{39}$$

where $\theta_0(\eta)$, $\theta_1(\eta)$ are given by Eqs. (37), (38), respectively, and constants appearing therein are given in the appendix. Here we omit the expression for $\theta_2(\eta)$ due to reasons of space. The expression for $\theta_1(\eta)$ and $\theta_2(\eta)$ are obtained with the help of the symbolic software MATHEMATICA. The perturbation solution given by (39) is applicable for small values of ε. However, for not-so-small ε, higher order approximations are warranted and in this paper we go up to three perturbation terms.

4.2.2. PHF case

In the PHF case we have

$$(1+\varepsilon g)g'' + Pr(fg' - \lambda f'g) + Pr(1+\varepsilon g)(\alpha f' + \beta g) + \varepsilon g'^2 = 0, \tag{40}$$

with the boundary conditions

$$\begin{aligned} & g'(\eta) = \tfrac{-1}{1+\varepsilon g(\eta)} \quad \text{at } \eta = 0, \\ & g(\eta) \to 0 \quad \text{as } \eta \to \infty. \end{aligned} \tag{41}$$

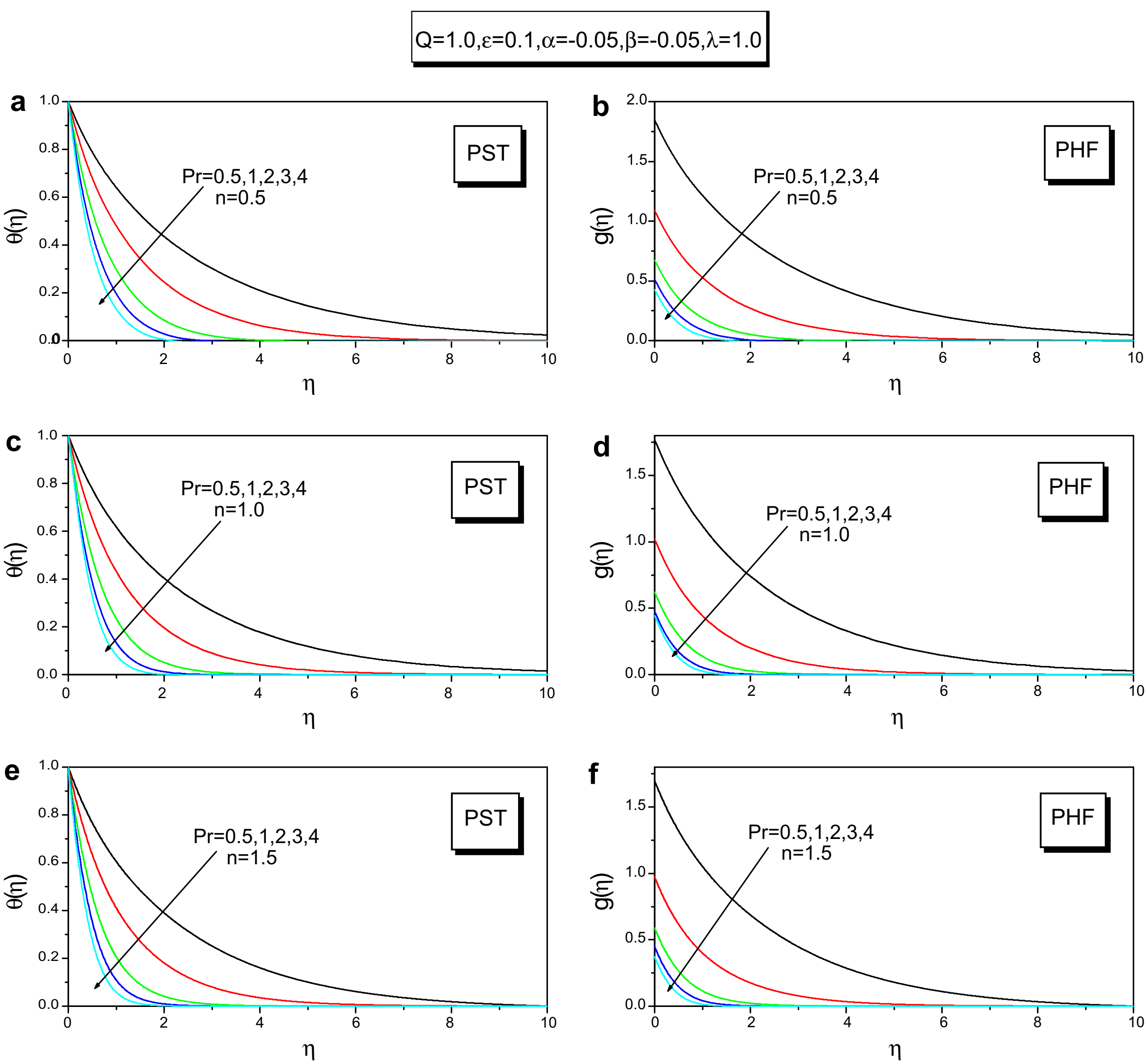

Fig. 6. Effect of Prandtl number *Pr* on temperature profiles.

Once again we adopt perturbation technique to solve Eq. (40) subject to the boundary conditions (41). The solution of Eq. (40) is assumed in the form

$$g(\eta) = g_0(\eta) + \varepsilon g_1(\eta) + \varepsilon^2 g_2(\eta) + \cdots \tag{42}$$

Following the same procedure we obtain the solution of the zeroth order perturbation equation in the form,

$$g_0(\eta) = \mathbb{C}_3 e^{-m\gamma\eta} M[\gamma - \lambda, b+1, -ae^{-m\eta}] + \left(\frac{\alpha}{1-a+a\beta}\right)\sum_{i=0}^{\infty}\left(\prod_{j=1}^{i}\frac{j-\lambda}{(j+1)^2 - a(j+1) + a\beta}\right)(-a)^{i+1}e^{-m(i+1)\eta} \tag{43}$$

Using (43), the solution of the first order perturbation equation is determined as,

$$\begin{aligned} g_1(\eta) = {} & \mathbb{C}_4 e^{-m\gamma\eta} M[\gamma - \lambda, b+1, -ae^{-m\eta}] \\ & + \{\tilde{a}_0 a^2 e^{-2m\eta} - \tilde{a}_1 a^3 e^{-3m\eta} + \tilde{a}_2 a^4 e^{-4m\eta} - \cdots\} \\ & + \mathbb{C}_3 e^{-m\gamma\eta}\{-\tilde{b}_0 a e^{-m\eta} + \tilde{b}_1 a^2 e^{-2m\eta} - \tilde{b}_2 a^3 e^{-3m\eta} + \cdots\} \\ & + \mathbb{C}_3^2 e^{-2m\gamma\eta}\{\tilde{c}_0 - \tilde{c}_1 a e^{-m\eta} + \tilde{c}_2 a^2 e^{-2m\eta} - \cdots\}. \end{aligned} \tag{44}$$

Similarly $g_2(\eta)$ is obtained. Finally the perturbation solution in the PHF case for small ε is written as

$$g(\eta) = g_0(\eta) + \varepsilon g_1(\eta) + \varepsilon^2 g_2(\eta), \tag{45}$$

where $g_0(\eta)$, $g_1(\eta)$ are given by Eqs. (43), (44) and constants appearing therein are listed in the appendix. Here also the expression for $g_2(\eta)$ is omitted due to reasons of space. The observation on the need of higher order approximations for not-so-small ε done in the context of PST holds for PHF also.

5. Results and discussion

MHD boundary layer flow and heat transfer in an electrically conducting power-law fluid over a stretching sheet with variable thermal conductivity is investigated in the presence of non-uniform heat source/sink. Analytical solutions are obtain for the special case $n = 1$ corresponding to Newtonian fluids. Numerical solution is warranted for the general case $n \neq 1$ which is achieved using the Keller box method. The effect of n, Q, Pr, α, β, ε and λ on flow and heat transfer are shown graphically in Figs. 3–10.

Fig. 3 depicts the effect of power-law index n and Chandrasekhar number Q on the horizontal velocity profiles $f'(\eta)$. It is a known fact

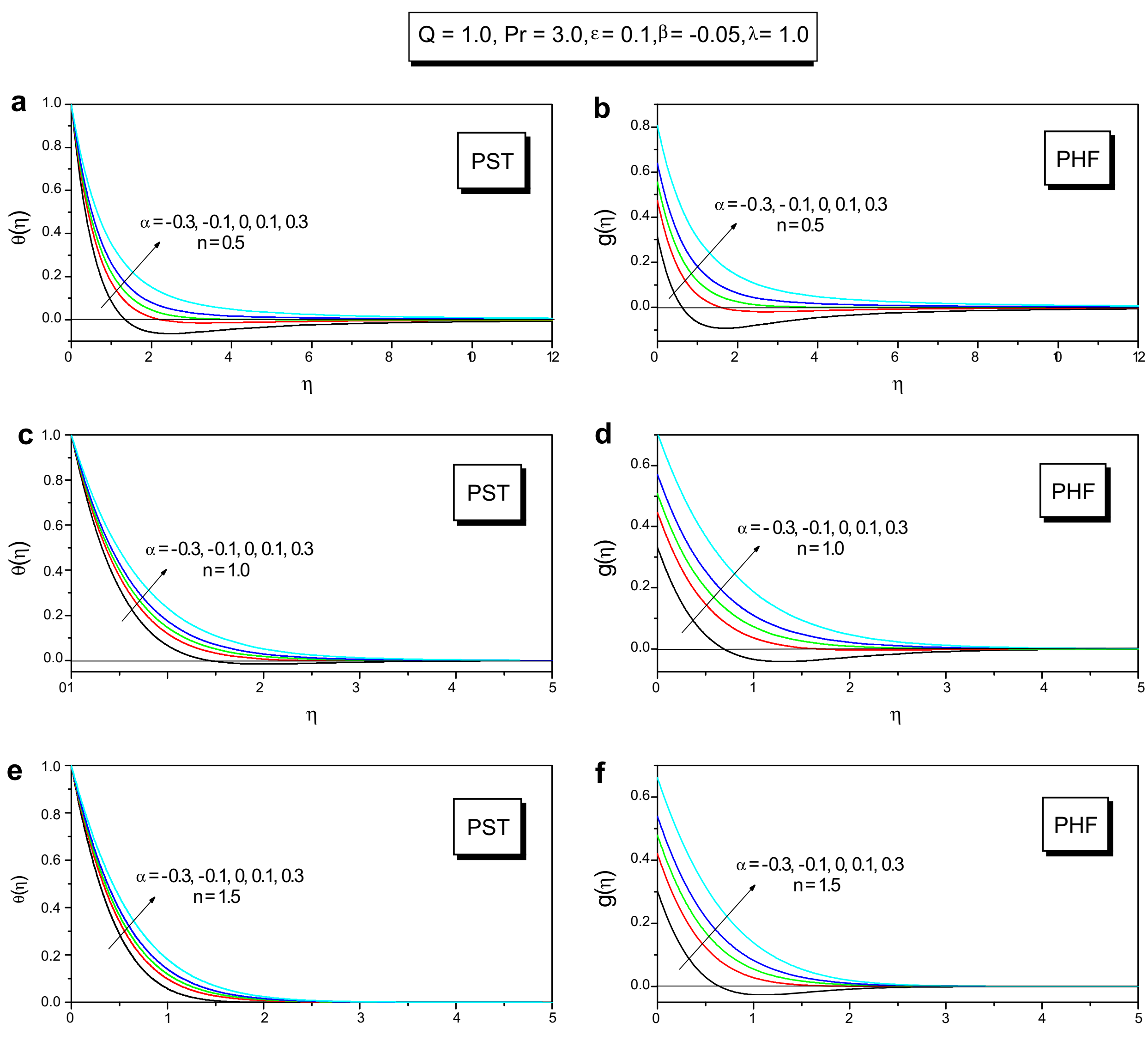

Fig. 7. Effect of space-dependent heat source/sink parameter α on temperature profiles.

that increasing values of n implies drag and thereby decrease in velocity. The same is reiterated by Fig. 3a. The effect of magnetic field is to flatten $f'(\eta)$ and the same is shown in Fig. 3b–d. The flattening of the profile is due to the applied transverse magnetic field that produces a Lorentz force, causing transverse contraction of the boundary layer. The magnetic field effect of flattening $f'(\eta)$ is same in pseudo-plastic, Newtonian and dilatant fluids.

Fig. 4 projects the influence of magnetic field on the skin friction parameter. From this graph it is evident that the skin friction parameter increases on the wall with increasing values of Q. This is expected as the applied magnetic field induces a retarding force (Lorentz force) against the motion of the fluid enhancing the drag.

The effect of transverse magnetic field on heat transfer is depicted in Fig. 5 for both PST and PHF cases. From these plots it is observed that the transverse magnetic field contributes to the thickening of thermal boundary layer. The resistance due to Lorentz force on the flow is responsible for enhancing the temperature in all the three cases: $0 < n < 1$, $n = 1$ and $n > 1$.

Fig. 6 shows the effect of Prandtl number on the heat transfer in the PST and PHF cases. From these plots it is evident that large values of Prandtl number result in thinning of the thermal boundary layer. This is in contrast to the effects of other parameters on heat transfer.

Fig. 7 illustrates the effect of space-dependent heat source/sink parameter α on the temperature profile for PST and PHF cases. It is observed that the thermal boundary layer generates energy which causes the temperature (in both PST and PHF) to increase in magnitude with increasing values of $\alpha(>0)$ whereas in the case $\alpha < 0$ boundary layer absorbs energy resulting a substantial fall in temperature with decreasing values of $|\alpha|$. It is observed in all these plots that the direction of the heat transfer is reversed for some negative values of α.

The effect of temperature-dependent heat source/sink parameter β on heat transfer is demonstrated in Fig. 8 for PST and PHF cases. These graphs show that energy is released for increasing values of $\beta(>0)$ and this causes the magnitude of temperature to increase both in PST and PHF cases, where as energy is absorbed for decreasing values of $\beta < 0$ resulting in the significant drop of temperature near the boundary layer.

The effect of variable thermal conductivity parameter ε on temperature profiles is shown in Fig. 9 for PST and PHF cases. It is observed from these plots that in the PST case the increasing values of ε result in increasing the magnitude of temperature causing thermal boundary layer thickening. This concurs with the results reported by Chiam [19,20]. In the PHF case an opposite effect is

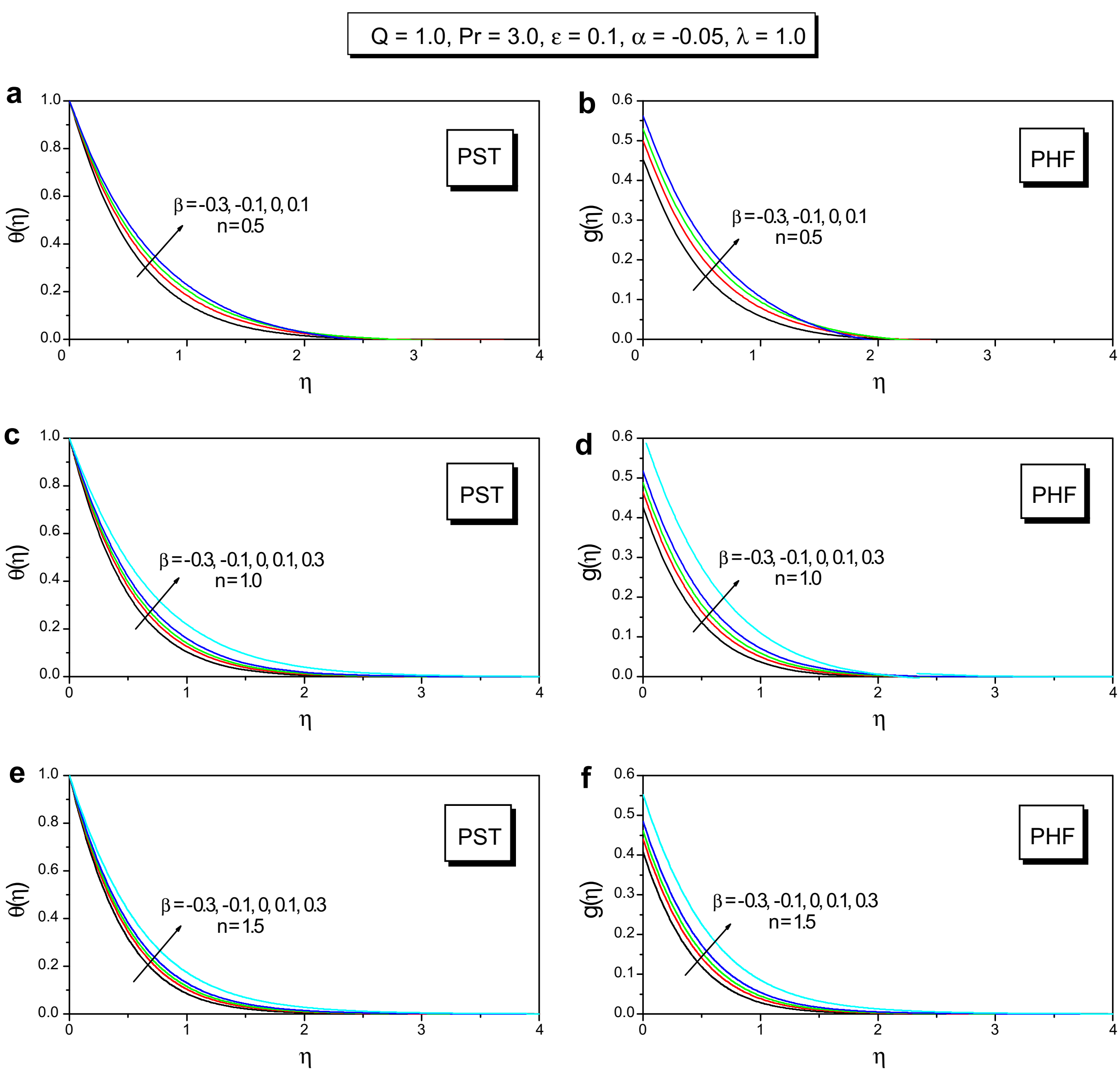

Fig. 8. Effect of temperature-dependent heat source/sink parameter β on temperature profiles.

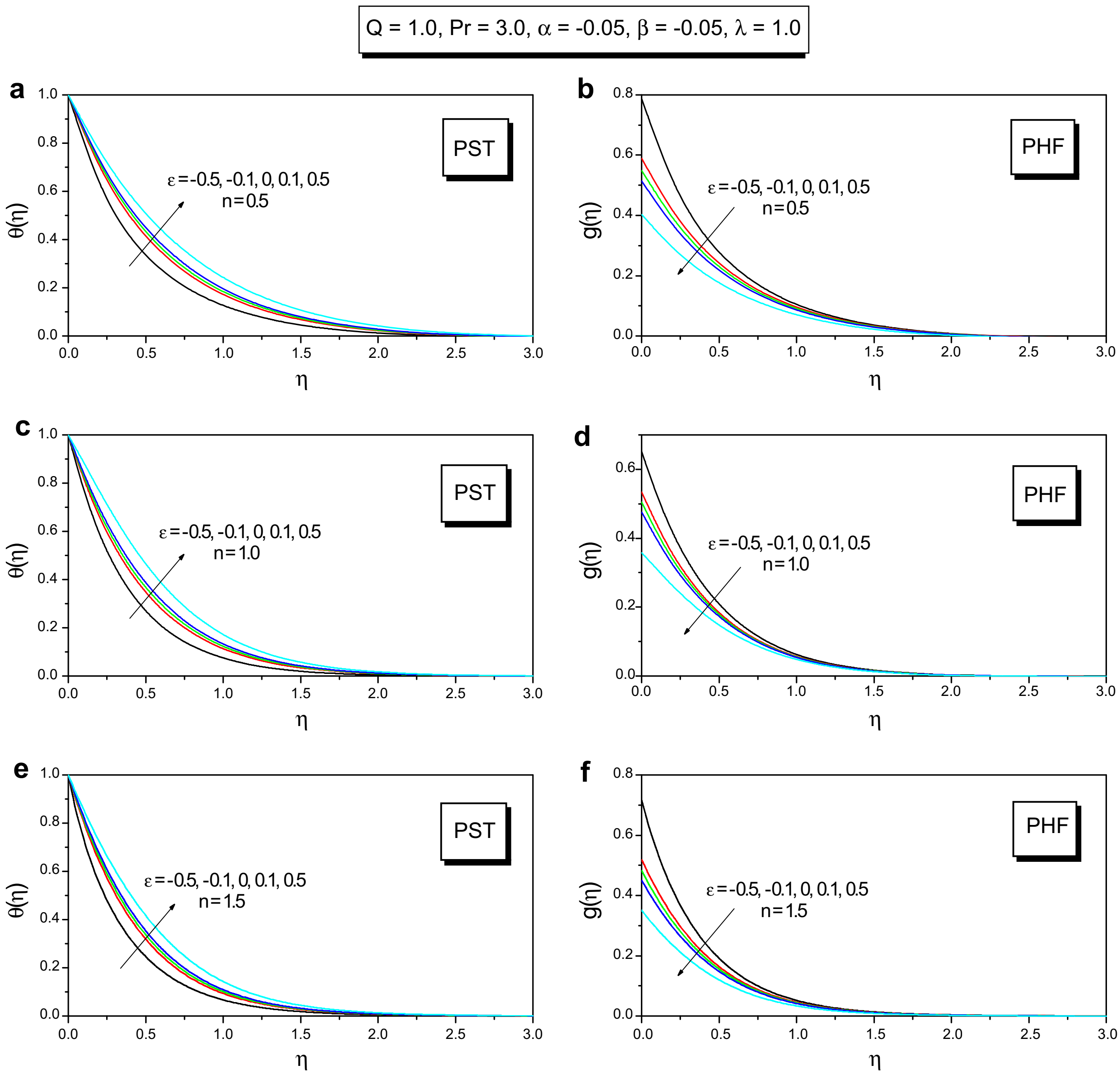

Fig. 9. Effect of thermal conductivity parameter ε on temperature profiles.

observed. It is also found that the wall temperature $g(0)$ shows steepening for non-so-small values of ε.

The effect of temperature parameter λ on the heat transfer is typical and is as in Grubka and Bobba [4]. Fig. 10 shows the effect of λ for PST and PHF cases. It is observed in both PST and PHF cases that above some critical negative value of λ, the increasing effect of λ is to decrease in the magnitude of the temperature. Below this negative value the effect of λ is opposite. For example, in the PST case the temperature gradient is negative for $\lambda > -0.049571818$ in respect of Newtonian fluid, and heat flows from the stretching sheet to the ambient fluid. When $\lambda = -0.049571818$, there is no heat transfer between the stretching surface and the ambient fluid. For $\lambda < -0.049571818$, the sign of the temperature gradient changes and heat flows from the fluid into the stretching surface. In the PHF case it is observed that the temperature gradient is negative for $\lambda < -1.001$ in respect of Newtonian fluid, and the heat diffuses from ambient fluid to the stretching surface, where as the opposite is true for $\lambda \geqslant -1.001$.The said effect is observed for all values of n but with different critical values of λ.

The values of $-f''(0)$, $-\theta'(0)$ and $g(0)$ are tabulated in Tables 1–3. Table 1 gives the comparison of $-f''(0)$ with Hassanien et al. [10], Cortell [26], Liao [30] and Anderson et al. [31]. We see that present results on $-f''(0)$ compare quite well with those of [10,26,30,31]. Table 2 gives the comparison of $-\theta'(0)$ with that of Chiam [20]. From this table it is observed that our numerical results coincide with the numerical results of Chiam [20] up to three decimal places. Our three term perturbation solution matches with the four term perturbation solution reported by Chiam [20] for small values of ε. However, for not-so-small values of ε higher order corrections are warranted. The values of $-\theta'(0)$ in case of PST and $g(0)$ in case of PHF are listed in Table 3 for various values of influencing parameters. Analyzing this table we infer that the effect increasing values of all the parameters except Pr and λ is to increase the values of $-\theta'(0)$ and $g(0)$ in pseudo-plastic Newtonian and dilatant fluids. The PHF bound-

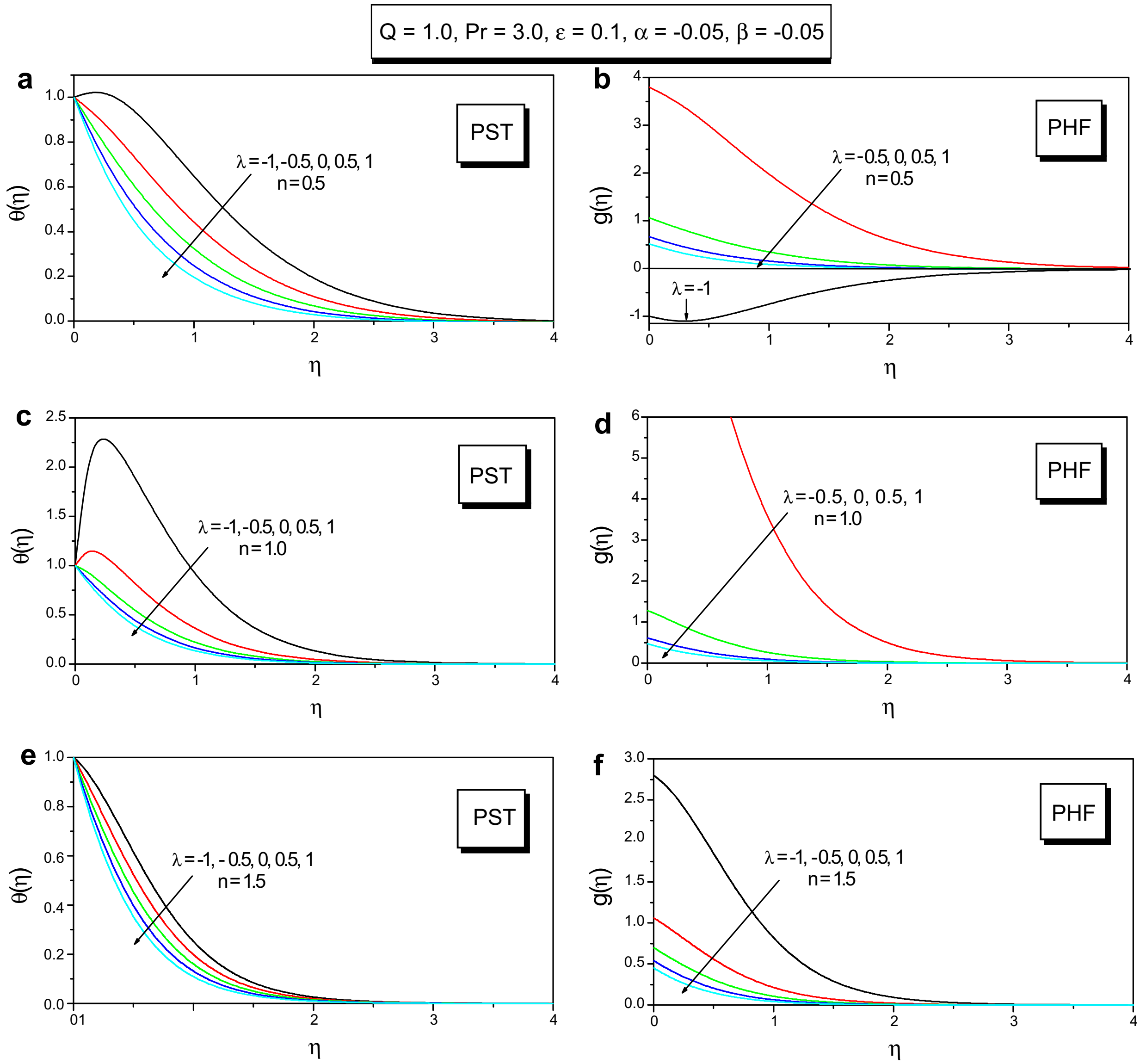

Fig. 10. Effect of wall temperature parameter λ on temperature profiles.

Table 1
Values of skin friction $-f''(0)$ for various values of power-law index n with $Q = 0$.

n	$-f''(0)$				
	Hassanien et al. [10]	Cortell [26]	Liao [30]	Andersson et al. [31]	Present study
0.2				1.9287	1.943695
0.4		1.2730		1.2715	1.272119
0.5	1.16524			1.1605	1.167740
0.6				1.0951	1.095166
0.8	1.02883		1.0280	1.0284	1.028713
1.0	1.00000	1.0000	1.0000	1.0000	1.000000
1.2	0.98737			0.9874	0.987372
1.4				0.9819	0.981884
1.5	0.98090		0.9820	0.9806	0.980653
1.6				0.9798	0.979827
1.8	0.97971			0.9794	0.979469
2.0		0.9797	0.9800	0.9800	0.979991

Table 2
Values of $\theta'(0)$ for various values ε with $Pr = n = 1, Q = \alpha = \beta = \lambda = 0$.

ε	Chiam [20]		Present study	
	Analytical $-\sum_{k=0}^{3}\varepsilon^k\theta'_k(0)$	Numerical $-\theta'(0)$	Analytical $-\sum_{k=0}^{2}\varepsilon^k\theta'_k(0)$	Numerical $-\theta'(0)$
0.0	0.5819767	0.5819767	0.5819767	0.5819767
0.01	0.5775551	0.5775650	0.5775653	0.5768627
0.05	0.5606327	0.5606773	0.5607232	0.5600819
0.1	0.5410215	0.5411268	0.5414776	0.5406564
0.2	0.5058168	0.5064329	0.5090105	0.5061888
0.3	0.4740012	0.4765327	**0.4845751**	0.4764906
0.4	0.4432131	0.4504452	**0.4681716**	0.4505875
0.5	0.4110909	0.4274450	**0.4597999**	0.4277759

Here, the bold numbers indicate that higher order corrections are warranted for not-so-small values of ε.

Table 3
Values of $-\theta'(0)$ and g(0) for various values $Q, Pr, \varepsilon, \alpha, \beta, \lambda$ and n.

Parameters	n = 0.5		n = 1.0		n = 1.5	
	$-\theta'(0)$	g (0)	$-\theta'(0)$	g (0)	$-\theta'(0)$	g (0)
Q	Pr = 3.0, α = −0.05, β = −0.05, λ = 1.0, ε = 0.1					
1.0	1.656164	0.514228	1.75704	0.47589	1.885245	0.450141
2.0	1.573416	0.544991	1.70304	0.49762	1.826902	0.466282
3.0	1.508367	0.571394	1.64179	0.51759	1.778368	0.480433
4.0	1.455418	0.594595	1.58573	0.53803	1.736485	0.493239
5.0	1.411287	0.615268	1.53694	0.55699	1.699523	0.505043
Pr	Q = 1.0, α = −0.05, β = −0.05, λ = 1.0, ε = 0.1					
0.5	0.526692	1.846620	0.54403	1.76846	0.566276	1.697526
1.0	0.839811	1.091951	0.88735	1.02043	0.931358	0.973748
2.0	1.300189	0.673081	1.39053	0.62192	1.471034	0.590956
3.0	1.656164	0.514228	1.75704	0.47589	1.885245	0.450141
4.0	1.955161	0.426618	1.53146	0.44590	2.232774	0.373022
α	Q = 1.0, Pr = 3.0, β = −0.05, λ = 1.0, ε = 0.1					
−0.3	1.974275	0.312598	1.96753	0.33237	2.154039	0.302574
−0.1	1.720133	0.473433	1.80249	0.44578	1.939194	0.420392
0.0	1.592020	0.555260	1.70992	0.50669	1.831202	0.480009
0.1	1.463205	0.638045	1.61066	0.57043	1.722827	0.540104
0.3	1.203448	0.806538	1.39203	0.70632	1.504924	0.661749
β	Q = 1.0, Pr = 3.0, α = −0.05, λ = 1.0, ε = 0.1					
−0.3	1.880886	0.453381	1.95629	0.42659	2.083412	0.407812
−0.1	1.704442	0.499868	1.79936	0.46447	1.927141	0.440454
0.0	1.606092	0.529832	1.71318	0.48834	1.841955	0.460623
0.1	1.504128	0.562072	1.61975	0.51718	1.750390	0.484548
0.3	1.403280	0.602345	1.39135	0.60502	1.536390	0.551978
λ	Q = 1.0, Pr = 3.0, α = −0.05, β = −0.05, ε = 0.1					
−1.0	0.427693	−0.997006	−18.6674	8662.52	0.402803	2.795688
−0.5	0.325687	3.797860	−3.56959	12.9774	0.863707	1.061513
0.0	0.866429	1.058423	0.19386	1.27708	1.251070	0.697585
0.5	1.295380	0.669511	1.29582	0.61719	1.587012	0.450141
1.0	1.656164	0.514228	1.75704	0.47589	1.656164	0.350779
ε	Q = 1.0, Pr = 3.0, α = −0.05, β = −0.05, λ = 1.0					
−0.5	2.974349	0.787063	2.74715	0.65169	3.334824	0.716607
−0.1	1.895578	0.589198	2.08708	0.53449	2.166057	0.518909
0.0	1.764810	0.549791	1.92206	0.50519	2.012728	0.482517
0.1	1.656164	0.514228	1.75704	0.47589	1.885245	0.450141
0.5	1.356256	0.402700	1.09697	0.35868	1.533163	0.350865

ary conditions are better suited than PST in cooling the stretching sheet relatively faster as can be seen from the tabulated values.

6. Conclusions

Some of the important findings of the paper are:

1. The effect of power-law index n and Chandrasekhar number Q is to decrease the momentum boundary layer thickness.
2. The individual and collective effects of increasing n, Q, α, and β are to increase the magnitude of heat transfer. The opposite effect is observed for increasing values of Pr and λ.
3. The variable thermal conductivity parameter ε increases the magnitude of temperature in PST case and decreases in PHF case. The wall temperature in the PHF case is dependent on the value of ε and shows steepening effect for not-so-small values of ε.
4. The magnitude of temperature parameter λ dictates the direction of heat transfer in both PST and PHF cases.
5. Comparison of results of PST and PHF boundary conditions reveals that PHF is better suited for effective cooling of the stretching sheet.

Acknowledgements

The authors are thankful to Department of Science and Technology, New Delhi, for providing financial support to carryout this work under the major research project (Grant No. SR/S4/MS: 198/03).

Appendix A

$$a = \frac{Pr}{m^2}, \quad b = \sqrt{a^2 - 4a\beta}, \quad \gamma = \frac{a+b}{2},$$

$$\tilde{a}_0 = \frac{\bar{a}_0}{4 - 2a + a\beta}, \quad \tilde{a}_i = \frac{\bar{a}_i + [(i+1) - \lambda]\tilde{a}_{i-1}}{(i+2)^2 - (i+2)a + a\beta}, \text{for } i = 1, 2, 3, \cdots$$

$$\tilde{b}_0 = \frac{\bar{b}_0}{(\gamma+1)^2 - (\gamma+1)a + a\beta}, \quad \tilde{b}_i = \frac{\bar{b}_i + [(\gamma+i) - \lambda]\tilde{b}_{i-1}}{(\gamma+i+1)^2 - (\gamma+i+1)a + a\beta}, \text{ for } i = 1, 2, 3, \cdots$$

$$\tilde{c}_0 = \frac{\bar{c}_0}{(2\gamma)^2 - (2\gamma)a + a\beta}, \quad \tilde{c}_i = \frac{\bar{c}_i + [(2\gamma+i-1) - \lambda]\tilde{c}_{i-1}}{(2\gamma+i)^2 - (2\gamma+i)a + a\beta}, \text{ for } i = 1, 2, 3, \cdots$$

$$\bar{a}_0 = b_0\alpha - (2 + a\beta)b_0^2,$$
$$\bar{a}_1 = b_1\alpha - (9 + 2a\beta)b_0b_1,$$
$$\bar{a}_2 = b_2\alpha - (8 + a\beta)(b_1^2 + 2b_0b_2),$$
$$\bar{a}_3 = b_3\alpha - (25 + 2a\beta)(b_1b_2 + b_0b_3),$$
$$\bar{a}_4 = b_4\alpha - (18 + a\beta)(b_2^2 + 2b_1b_3 + 2b_0b_4), \cdots \text{ and so on}$$
$$\bar{b}_0 = a_0\alpha - \{(\gamma+1)^2 + 2a\beta\}a_0b_0,$$
$$\bar{b}_1 = a_1\alpha - \{(\gamma+2)^2 + 2a\beta\}(a_0b_1 + a_1b_0),$$
$$\bar{b}_2 = a_2\alpha - \{(\gamma+3)^2 + 2a\beta\}(a_0b_2 + a_1b_1 + a_2b_0),$$
$$\bar{b}_3 = a_3\alpha - \{(\gamma+4)^2 + 2a\beta\}(a_0b_3 + a_1b_2 + a_2b_1 + a_3b_0),$$
$$\bar{b}_4 = a_4\alpha - \{(\gamma+5)^2 + 2a\beta\}(a_0b_4 + a_1b_3 + a_2b_2 + a_3b_1 + a_4b_0), \cdots \text{ and so on}$$
$$\bar{c}_0 = -(2\gamma^2 + a\beta)a_0^2,$$
$$\bar{c}_1 = -\{(1+2\gamma)^2 + 2a\beta\}a_0a_1,$$
$$\bar{c}_2 = -\{2(1+\gamma)^2 + a\beta\}(a_1^2 + 2a_0a_2),$$
$$\bar{c}_3 = -\{(3+2\gamma)^2 + 2a\beta\}(a_1a_2 + a_0a_3),$$
$$\bar{c}_4 = -\{2(2+\gamma)^2 + a\beta\}(a_2^2 + 2a_1a_3 + 2a_0a_4), \cdots \text{ and so on}$$
$$a_0 = 1, \quad a_1 = \frac{(\gamma-\lambda)}{(b+1)1!}, \quad a_2 = \frac{(\gamma-\lambda)(\gamma-\lambda+1)}{(b+1)(b+2)2!}, \cdots \text{ and so on}$$
$$b_0 = \left(\frac{\alpha}{1 - a + a\beta}\right), \quad b_i = \left(\prod_{j=1}^{i} \frac{j - \lambda}{(j+1)^2 - a(j+1) + a\beta}\right)b_0, \quad i = 1, 2, 3\cdots$$

$$\mathbb{C}_1 = \frac{1 - \left(\frac{\alpha}{1-a+a\beta}\right)\sum_{i=0}^{\infty}\left(\prod_{j=1}^{i}\frac{j-\lambda}{(j+1)^2 - a(j+1) + a\beta}\right)(-a)^{i+1}}{M[\gamma - \lambda, b+1, -a]},$$

$$\mathbb{C}_2 = \frac{-\{s_1 + \mathbb{C}_1 s_2 + \mathbb{C}_1^2 s_3\}}{M[\gamma - \lambda, b+1, -a]},$$

$$\mathbb{C}_3 = \frac{\frac{1}{m} - \left(\frac{\alpha}{1-a+a\beta}\right)\sum_{i=0}^{\infty}\left(\prod_{j=1}^{i}\frac{j-\lambda}{(j+1)^2 - a(j+1) + a\beta}\right)(i+1)(-a)^{i+1}}{\{\gamma M[\gamma - \lambda, b+1, -a] - \frac{a(\gamma-\lambda)}{b+1}M[\gamma - \lambda + 1, b+2, -a]\}}$$

$$\mathbb{C}_4 = \frac{-\{\frac{g_0(0)}{M} + t_1 + \mathbb{C}_3 t_2 + \mathbb{C}_3^2 t_3\}}{\left\{\gamma M[\gamma - \lambda, b+1, -a] - \frac{a(\gamma-\lambda)}{b+1}M[\gamma - \lambda + 1, b+2, -a]\right\}}$$

$$s_1 = \tilde{a}_0a^2 - \tilde{a}_1a^3 + \tilde{a}_2a^4 - \tilde{a}_3a^5 + \cdots$$
$$s_1 = -\tilde{b}_0a + \tilde{b}_1a^2 - \tilde{b}_2a^3 + \tilde{b}_3a^4 - \cdots$$
$$s_3 = \tilde{c}_0 - \tilde{c}_1a + \tilde{c}_2a^2 - \tilde{c}_3a^3 + \cdots$$
$$t_1 = 2\tilde{a}_0a^2 - 3\tilde{a}_1a^3 + 4\tilde{a}_2a^4 - 5a\tilde{a}_3a^5 + \cdots$$
$$t_2 = -(\gamma+1)\tilde{b}_0a + (\gamma+2)\tilde{b}_1a^2 - (\gamma+3)\tilde{b}_2a^3 + (\gamma+4)\tilde{b}_3a^4 - \cdots$$
$$t_3 = (2\gamma)\tilde{c}_0 - (2\gamma+1)\tilde{c}_1a + (2\gamma+2)\tilde{c}_2a^2 - (2\gamma+3)\tilde{c}_3a^3 + \cdots$$

References

[1] L.J. Crane, Flow past a stretching sheet, ZAMP 21 (1970) 645–647.
[2] P.S. Gupta, A.S. Gupta, Heat and mass transfer on a stretching sheet with suction or blowing, Can. J. Chem. Eng. 55 (1977) 744–746.
[3] C.K. Chen, M.I. Char, Heat transfer of a continuous stretching surface with suction or blowing, J. Math. Anal. Appl. 135 (1988) 568–580.
[4] L.J. Grubka, K.M. Bobba, Heat transfer characteristics of a continuous stretching surface with variable temperature, ASME J. Heat Transfer 107 (1985) 248–250.
[5] T.C. Chiam, Magnetohydrodynamic heat transfer over a non-isothermal stretching sheet, Acta Mech. 122 (1997) 169–179.
[6] A. Acrivos, M.J. Shah, E.E. Peterson, Momentum and heat transfer in laminar boundary layer flows of non-Newtonian fluids past external surfaces, AIChE J. 6 (1960) 312–316.
[7] W.R. Schowalter, The application of boundary layer theory to power law pseudo plastic fluids: similar solutions, AIChE J. 6 (1960) 24–28.
[8] H.I. Andersson, B.S. Dandapat, Flow of a power law fluid over a stretching sheet, Stability Appl. Anal. Continuous Media 1 (1991) 339–347.
[9] M.A.A. Mahmoud, M.A.E. Mahmoud, Analytical solutions of hydromagnetic boundary layer flow of a non-Newtonian power law fluid past a continuously moving surface, Acta Mech. 181 (2006) 83–89.
[10] I.A. Hassanien, A.A. Abdullah, R.S. Gorla, Flow and heat transfer in a power-law fluid over a non-isothermal stretching sheet, Math. Comput. Model. 28 (9) (1998) 105–116.
[11] T. Sarpakaya, Flow of non-Newtonian fluids in a magnetic field, AIChE J. 7 (1961) 324–328.
[12] H.I. Andersson, MHD flow of a viscoelastic fluid past a stretching surface, Acta Mech. 95 (1992) 227–230.
[13] P.G. Siddheshwar, U.S. Mahabaleshwar, Effect of radiation and heat source on MHD flow of a viscoelastic liquid and heat transfer over a stretching sheet, Int. J. Non-Linear Mech. 40 (2005) 807–820.
[14] Emad M. Abo-Eldahab, Ahmed M. Salem, MHD free-convection flow of a non-Newtonian power-law fluid at a stretching surface with a uniform free-stream, Appl. Math. Comput. 169 (2005) 806–818.
[15] K. Vajravelu, D. Rollins, Heat transfer in electrically conducting fluid over a stretching surface, Int. J. Non-Linear Mech. 27 (2) (1992) 265–277.
[16] K. Vajravelu, J. Nayfeh, Convective heat transfer at a stretching sheet, Acta Mech. 96 (1993) 47–54.
[17] Emad M. Abo-Eldahab, Mohamed A. El Aziz, Blowing/suction effect on hydromagnetic heat transfer by mixed convection from an inclined continuously stretching surface with internal heat generation/absorption, Int. J. Therm. Sci. 43 (2004) 709–719.
[18] W.M. Kays, M.E. Grawford, Convection Heat and Mass Transfer, Pergamon, Oxford, 1980.
[19] T.C. Chiam, Heat transfer with variable conductivity in a stagnation-point flow towards a stretching sheet, Int. Commun. Heat Mass Transfer 23 (1996) 239–248.
[20] T.C. Chiam, Heat transfer in a fluid with variable thermal conductivity over a linearly stretching sheet, Acta Mech. 129 (1998) 63–72.
[21] A. Subhas, K.V. Prasad, Ali Mahaboob, Buoyancy force and thermal radiation effects in MHD boundary layer viscoelastic flow over continuously moving stretching surface, Int. J. Therm. Sci. 44 (2005) 465–476.
[22] R.B. Bird, W.E. Stewart, E.N. Lightfoot, Transport Phenomena, John Wiley, New York, 1960.
[23] M. Abramowitz, L.A. Stegun, Handbook of Mathematical Functions, National Bureau of Standards/Amer. Math. Soc., Providence, RI, vol. 55, 1972.
[24] S.D. Conte, C. de Boor, Elementary Numerical Analysis, McGraw-Hill, New York, 1972.
[25] T. Cebeci, P. Bradshaw, Physical and Computational Aspects of Convective Heat Transfer, Springer-Verlag, New York, 1984.
[26] R. Cortell, A note on magnetohydrodynamic flow of a power-law fluid over a stretching sheet, Appl. Math. Comput. 168 (2005) 557–566.
[27] M.S. Abel, P.G. Siddheshwar, M.M. Nandeppanavar, Heat transfer in a viscoelastic fluid past a stretching sheet with non-uniform heat source, Int. J. Heat Mass Transfer 50 (2007) 960–966.
[28] M.S. Abel, N. Mahesha, Heat transfer in MHD viscoelastic fluid flow over a stretching sheet with variable thermal conductivity, non-uniform heat source and radiation, Appl. Math. Model. 32 (2008) 1965–1983.
[29] S.J. Liao, A uniformly valid analytic solution of 2D viscous flow past a semi-infinite flat plate, J. Fluid Mech. 385 (1999) 101–128.
[30] S.J. Liao, On the analytic solution of magnetohydrodynamic flows of non-Newtonian fluids over a stretching sheet, J. Fluid Mech. 488 (2003) 189–212.
[31] H.I. Andersson, V. Kumaran, On sheet-driven motion of power-law fluids, Int. J. Non-Linear Mech. 41 (2006) 1228–1234.
[32] K.R. Rajagopal, T.Y. Na, A.S. Gupta, Flow of a visco-elastic fluid over a stretching sheet, Rheol. Acta 23 (1984) 213–215.
[33] K.B. Pavlov, Magnetohydrodynamic flow of an impressible viscous fluid caused by deformation of a surface, Magnitnaya Gidrodinamika 4 (1974) 146–147.